

Comparison of HCV-associated gene expression and cell signaling pathways in cells with or without HCV replicon and in replicon-cured cells

Yuki Nishimura-Sakurai · Naoya Sakamoto · Kaoru Mogushi · Satoshi Nagaie · Mina Nakagawa · Yasuhiro Itsui · Megumi Tasaka-Fujita · Yuko Onuki-Karakama · Goki Suda · Kako Mishima · Machi Yamamoto · Mayumi Ueyama · Yusuke Funaoka · Takako Watanabe · Seishin Azuma · Yuko Sekine-Osajima · Sei Kakinuma · Kiichiro Tsuchiya · Nobuyuki Enomoto · Hiroshi Tanaka · Mamoru Watanabe

Received: 2 September 2009 / Accepted: 2 November 2009 / Published online: 12 December 2009
© Springer 2009

Abstract

Background Hepatitis C virus (HCV) replication is affected by several host factors. Here, we screened host genes and molecular pathways that are involved in HCV replication by comprehensive analyses using two genotypes of HCV replicon-expressing cells, their *cured* cells and naïve Huh7 cells.

Y. Nishimura-Sakurai and N. Sakamoto contributed equally to this work.

Electronic supplementary material The online version of this article (doi:10.1007/s00535-009-0162-3) contains supplementary material, which is available to authorized users.

Y. Nishimura-Sakurai · N. Sakamoto (✉) · M. Nakagawa · Y. Itsui · M. Tasaka-Fujita · Y. Onuki-Karakama · G. Suda · K. Mishima · M. Yamamoto · M. Ueyama · Y. Funaoka · T. Watanabe · S. Azuma · Y. Sekine-Osajima · S. Kakinuma · K. Tsuchiya · M. Watanabe
Department of Gastroenterology and Hepatology,
Tokyo Medical and Dental University, 1-5-45 Yushima,
Bunkyo-ku, Tokyo 113-8519, Japan
e-mail: nsakamoto.gast@tmd.ac.jp

N. Sakamoto · M. Nakagawa · S. Kakinuma
Department for Hepatitis Control,
Tokyo Medical and Dental University, Tokyo, Japan

K. Mogushi · S. Nagaie · H. Tanaka
Information Center for Medical Science,
Tokyo Medical and Dental University, Tokyo, Japan

Y. Itsui
Department of Internal Medicine,
Soka Municipal Hospital, Saitama, Japan

N. Enomoto
First Department of Internal Medicine,
University of Yamanashi, Yamanashi, Japan

Methods Huh7 cell lines that stably expressed HCV genotype 1b or 2a replicon were used. The *cured* cells were established by treating HCV replicon cells with interferon- α . Expression of 54,675 cellular genes was analyzed by GeneChip DNA microarray. The data were analyzed by using the KEGG Pathway database.

Results Hierarchical clustering analysis showed that the gene-expression profiles of each cell group constituted clear clusters of naïve, HCV replicon-expressed, and cured cell lines. The pathway process analysis between the replicon-expressing and the *cured* cell lines identified significantly altered pathways, including MAPK, steroid biosynthesis and TGF- β signaling pathways, suggesting that these pathways were affected directly by HCV replication. Comparison of *cured* and naïve Huh7 cells identified pathways, including steroid biosynthesis and sphingolipid metabolism, suggesting that these pathways were required for efficient HCV replication. Cytoplasmic lipid droplets were obviously increased in replicon-expressing and *cured* cells as compared to naïve cells. HCV replication was significantly suppressed by peroxisome proliferator-activated receptor (PPAR)- α agonists but augmented by PPAR- γ agonists.

Conclusion Comprehensive gene expression and pathway analyses show that lipid biosynthesis pathways are crucial to support proficient virus replication. These metabolic pathways could constitute novel antiviral targets against HCV.

Keywords DNA microarray · KEGG database · HCV replicon · Lipid metabolism

Abbreviations

HCV Hepatitis C virus
TLR Toll-like receptor
BMP Bone morphogenetic protein

TGF	Transforming growth factor
FKBP	FK-binding protein
HSP	Heat shock proteins
FBS	Fetal bovine serum
YFP	Yellow fluorescence protein
FACS	Fluorescent activated cell sorting
RIN	RNA integrity number
SAM	Significance analysis of microarray
KEGG	Kyoto Encyclopedia of Genes and Genomes
EGID	NCBI Entrez Gene ID
RT-PCR	Reverse transcription-polymerase chain reaction
MTS	Dimethylthiazol carboxymethoxyphenyl sulfophenyl tetrazolium
PPAR	Peroxisome proliferator-activated receptor

Introduction

Hepatitis C virus (HCV) infection is one of the most important causative agents of acute and chronic hepatitis, liver cirrhosis and hepatocellular malignancies [1]. Currently, the most efficient combination treatment of ribavirin plus peginterferon can eliminate the virus in almost half of the patients treated [2, 3]. Thus, it is our high priority goal to understand the HCV life cycle precisely, to identify cellular cofactors for HCV replication and to develop new class antiviral therapeutics.

Molecular analyses of the HCV life cycle, virus–host interactions, and mechanisms of liver cell damage by the virus are not understood completely, mainly because of the lack of cell culture systems. These problems have been partly overcome by the development of the HCV subgenomic replicon [4] and HCV cell culture systems [5, 6]. These systems have allowed us to study the complete HCV life cycle: virus-cell entry, translation, protein processing, RNA replication, virion assembly and virus release.

Several host proteins and drugs have been reported to have a direct effect on HCV replication in vitro [7]. These include factors that affect immune responses (interferons and their related genes [8, 9], RIG-I, TLRs [10]), cell proliferation (BMP7 [11], TGF-beta [12], nucleolin [13]), molecular chaperone function (cyclophilin [14], ER-stress proteins [15], FKBP [16], HSP27 [17], HSP90 [18]) and lipid metabolism (cholesterol, sphingolipid [19]). However, it is often difficult to determine whether these genes are changed by HCV replication or the changes are essential for HCV replication in the host cells.

In this study, we investigated the effects of host cellular gene expression using our HCV replicon system [20, 21]. We performed DNA microarray analyses using cells expressing the replicons, the corresponding *cured* cells, from which the replicon had been eliminated by prolonged treatment with interferon-alpha, and naïve Huh7 cells. Furthermore, we investigated the signaling pathways using DNA microarrays to study molecular pathways that are involved in the HCV life cycle and its pathogenesis.

Materials and methods

Cells and cell culture

Huh7 cells were maintained in Dulbecco's modified minimal essential medium (Sigma, St. Louis, MO) supplemented with 10% fetal calf serum at 37°C under 5% CO₂. To maintain cell lines carrying the HCV replicon (Huh7/Rep cells), G418 (Nakalai Tesque, Kyoto, Japan) was added to the culture medium to a final concentration of 500 µg/ml.

HCV replicon and cell culture

The HCV-1b replicon plasmid, pHCV1bneo-delS, was provided by Dr. Christoph Seeger (Fox Chase Cancer Center, Philadelphia, PA) [22]. HCV-2a replicon plasmid, pSGR-JFH1, was provided by Dr. Takaji Wakita (National Institute of Infectious Diseases, Tokyo, Japan). The neomycin phosphotransferase (Neo) gene of pHCV1bneo-delS and pSGR-JFH1 was replaced by a chimeric gene coding for yellow fluorescent protein fused in-frame with the foot-and-mouth disease virus peptide 2A (P2A) autocleavage motif followed by neomycin phosphotransferase, which we designated *Yeo* (Fig. 1) [23]. An HCV *Yeo*-replicon that expresses chimeric firefly luciferase and the neomycin resistance gene has been described [20, 21]. In vitro replicon RNA synthesis, RNA transfection and selection of G418-resistant cell lines were carried out as described previously [21, 24]. Briefly, replicon RNAs were transfected into Huh7 cells. By cell culture in the presence of G418, we established Huh7 cell lines that stably express the *Yeo*-replicons: Huh7/Rep-1b-*Yeo* and Huh7/Rep-2a-*Yeo*.

Fluorescence microscopy and FACS analysis

The cells were plated onto eight-well chamber slides (Lab-Tek® Chamber Slide™ System, Nalgen Nunc International, Rochester, NY), and the YFP expression was detected by fluorescence microscopy (BZ-8000,

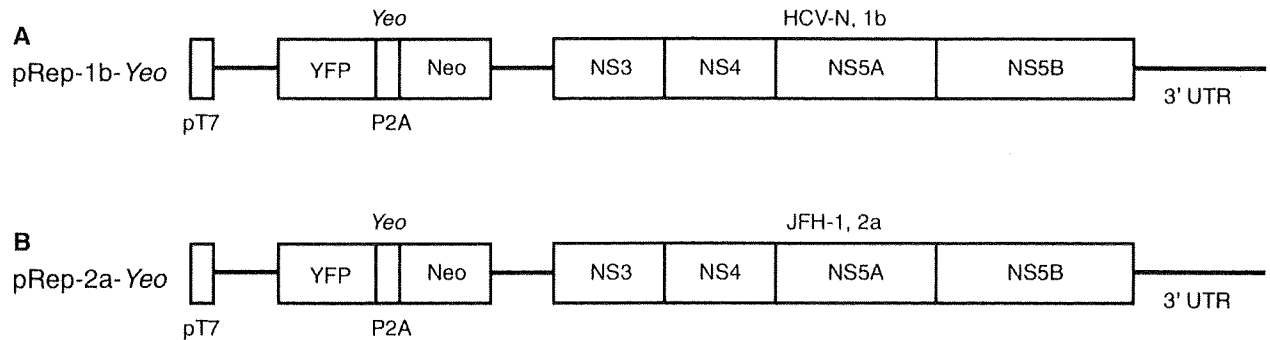


Fig. 1 Structure of replicon plasmid constructs. A hepatitis C virus (HCV) replicon plasmid, pRep-1b-Yeo (a) and pRep-2a-Yeo (b), was reconstructed from pHCV1bneo-delS [22] and pSGR-JFH1 [47] by replacing the neomycin phosphotransferase (Neo) gene with a fusion

gene of yellow fluorescence protein (YFP) and Neo, which we designate “Yeo.” NS Nonstructural region, *pT7* T7 promoter, *3'UTR* 3'untranslated region, *P2A* foot-and-mouth disease peptide 2A (see also “Materials and methods”) [23]

KEYENCE, Osaka, Japan) and FACS Caliber using CellQuest software (BD Biosciences, Franklin Lakes, NJ).

Cell sorting

Cells were treated for 5 min with trypsin/EDTA at 37°C and then resuspended in 10% FBS/DMEM. A single cell suspension was prepared by passage through a 35- μ m nylon filter. The cell populations that support a high level of Yeo-replicon expression (Huh7/Rep-1b-Yeo^{high} and Huh7/Rep-2a-Yeo^{high}) were separated using a FACS Vantage SE cell-sorting system (BD Biosciences). The YFP-directed fluorescence of sorted cells was confirmed by fluorescence microscopy and FACS.

Establishment of the cured Huh7 cells

Cured Huh7 cells (cHuh7) were established by eliminating the HCV replicon from the Yeo-1b^{high} and -2a^{high} replicon expressing Huh7 cells by treatment with 100 U/ml of interferon-alpha for 14 days [6, 25]. Clearance of replicon RNA was confirmed by FACS analysis and by the loss of resistance to G418.

RNA preparation and microarray hybridization

Total cellular RNA was extracted from the 1b^{high} and 2a^{high} Yeo-replicon cells, cured-1b and -2a cells and naïve Huh7 cells using ISOGEN (Wako). Integrity of obtained RNA was assessed using Agilent 2100 Bioanalyzer (Agilent Technologies, Palo Alto, CA). All samples had an RNA Integrity Number (RIN) greater than 9.4 [26]. Complementary RNA was prepared from 1 μ g total RNA, using one-cycle target labeling and a control reagents kit (Affymetrix, Santa Clara, CA). Hybridization and signal detection of the Human Genome U133 Plus 2.0 array (Affymetrix) were performed in accordance with the

manufacturer's instructions. Assays were performed in duplicate.

Analysis of gene expression data

A total of ten microarray datasets was normalized using the robust multi-array average (RMA) method under R 2.8.1 statistical software (<http://www.R-project.org>). Estimated gene expression levels were \log_2 -transformed, data from 62 control probe sets were removed, and we selected 18,613 probe sets that were categorized as “present” or “marginal” among all samples. We performed two sets of gene comparisons to examine effects of HCV replicons on host cellular gene expression: one was the high Yeo-replicon-expressing cells versus cured cells and the other was parental Huh7 cells versus cured cells. We selected differentially expressed genes using the significance analysis of microarray (SAM) as described by Tusher et al. [27], and the fold changes and the *Q*-values were calculated for each probe sets. We used $\delta = 0.1$ as a cutoff parameter for SAM. A hierarchical clustering with selected genes was performed with R software. Euclidean distance was used to calculate the similarity matrix among genes or cell conditions, respectively. The complete linkage method was used for agglomeration.

Molecular pathway analysis and visualization of gene expression data

We used the KEGG Pathway database to investigate the molecular reactions and pathways that showed significant gene expression changes [28]. The KEGG Pathway is a database of biological systems, consisting of over 4,252 genes and 204 molecular pathway-wiring diagrams of interaction and reaction networks (<http://www.genome.jp/kegg/pathway.html>). Prior to the pathway analysis, we selected probe sets that were differentially expressed

between Huh7 and *cured* cells and between *cured* cells and replicon cells. For Huh7 versus *cured* cells analyses, we selected probe sets that showed 20% upregulation or downregulation (i.e., fold change of greater than 1.2) in both Huh7 versus *cured*-1b and Huh7 versus *cured*-2a cells. For replicon cell versus *cured* cell analyses, we selected probe sets that showed 20% upregulation or downregulation in both *cured*-1b versus replicon-1b cells or *cured*-2a versus replicon-2a cells. Association between the obtained gene list and each pathway was evaluated by Fisher's exact test. The significance level for KEGG analysis was set to a false discovery rate (FDR) of lower than 0.3 using the Benjamini and Hochberg method [29].

We next visualized functional associations between the differentially expressed genes and biological pathway processes. The KEGG Pathway provides a reference knowledge base for linking genomes to biological systems and also to environments by the processes of Pathway mapping and BRITe mapping. NCBI Entrez Gene IDs (EGIDs) for each gene in the pathways were extracted from the database. The relationship between probe sets on the microarray and EGIDs was obtained from a gene annotation file provided by Affymetrix. Thereafter, gene expression changes were mapped on the pathway by combining the results of fold-change analyses with the data sets above.

Real-time PCR analysis of mRNA expression

To confirm the results of the microarray analysis, we examined the expression levels of several mRNA by real-time RT-PCR (7500 Real Time PCR Systems, Applied Biosystems, Foster City, CA). Single-stranded cDNA was synthesized from total RNA using SuperScript II reverse transcriptase (Invitrogen) and random hexamers (Takara Bio Inc., Shiga, Japan) as primers. Expression of mRNA was quantified using QuantiTect SYBR Green PCR master Mix (QIAGEN, Valencia, CA). The primers used were as follows: HMGCR, SQLE, CYP51A1, TM7SF2, NSDHL, EBP and beta-actin. The nucleotide sequences of primers and corresponding product sizes are as indicated (see Supplementary Table 1).

Oil red O staining

Huh7 cells, replicon cells and *cured* cells were cultured on 18-mm-round micro cover glasses (Matsunami, Tokyo, Japan). These cells were fixed with 4% paraformaldehyde for 5 min at room temperature. After washing with PBS, the cells were permeabilized with 0.05% Triton X-100 in PBS for 5 min at room temperature. Staining of intracellular neutral lipids was performed with Oil red O, and nuclei were stained with Mayer's hematoxylin using Oil

red O stain kit procedure (Diagnostic Biosystems Inc., Pleasanton, CA).

Immunofluorescence analysis

Huh7 cells, replicon cells and *cured* cells were cultured on 18-mm-round micro cover glasses. For immunostaining, the cells were fixed in 4% paraformaldehyde for 5 min at room temperature. For detection of HCV-NS5A, cells were incubated with the primary antibody (Bioscience International, Saco, ME) for 1 h at 37°C. The fluorescent secondary antibodies were Alexa Fluor 594 goat anti-mouse IgG antibody (Invitrogen, Carlsbad, CA). Nuclei were labeled with 4',6-diamidino-2-phenylindole (DAPI). Lipid droplets were visualized with BODIPY 493/503 (Invitrogen). Analysis was performed on a Delta-Vision microscope system (Applied Precision, Seattle, WA).

Luciferase-based expression analysis of HCV replicon and analysis of cell viability

Huh7/Rep-Feo cells [20, 21] were cultured with various concentrations of peroxisome proliferator-activated receptor (PPAR)-alpha and -gamma agonists. After 48 h of culture, levels of HCV replication were quantified by internal luciferase assay using a Bright-Glo Luciferase Assay System (Promega). Assays were performed in triplicate, and the results were expressed as mean \pm SD as percentages of the controls. To evaluate cell viability, dimethylthiazol carboxymethoxyphenyl sulfophenyl tetrazolium (MTS) assay was performed using a Cell Titer 96 Aqueous One Solution Cell Proliferation Assay (Promega) according to manufacturer's directions.

Statistical analyses

Statistical analyses were performed using the Student's *t*-test, and *P*-values of less than 0.05 were considered as statistically significant.

Results

Fluorescence detection of Yeo replicon

Genotypes 1b and 2a Yeo-replicon RNAs were stably transfected into Huh7 cells (Huh7/Rep-1b-Yeo and Huh7/Rep-2a-Yeo, respectively, Fig. 1). In these transfected cells, expression of the HCV replicon was visualized by HCV-IRES-driven, YFP-mediated fluorescence (Fig. 2, left panels). The expression levels of individual cells could be measured by fluorescence intensity and cytogram analysis using flow cytometry (Fig. 2, right panels).

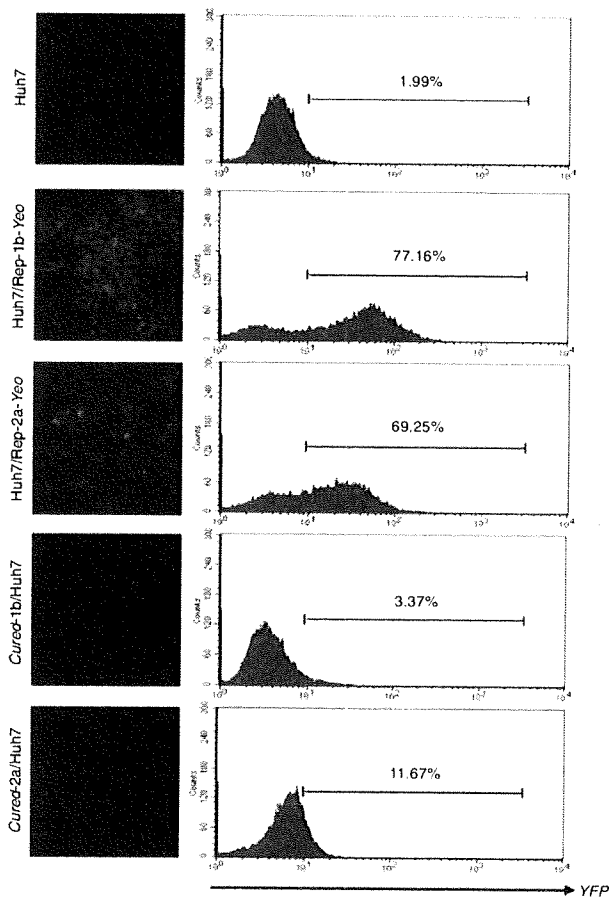


Fig. 2 Visualization of YFP replicon expression. Detection of YFP expression by fluorescence microscopy analysis and of intracellular YFP expression by FACS analysis

Our initial trial was to compare gene expression profiles between replicon-expressing cells and parental Huh7 cells. However, these comparisons identified gene expressional changes induced by HCV infection and by adaptation of the host cell to support efficient HCV replication, because transfection of replicon RNA and G418-treatment of cells resulted in selection of a cell population that can support a high level of HCV subgenomic replication. Therefore, we used *cured* cell lines, which were established from Huh7/Rep-1b-Yeo and -2a-Yeo by interferon-alpha treatment. These cured cell lines are highly permissive for HCV replication on re-introduction of virus or replicon RNA (Fig. 2). With these backgrounds, we performed two sets of gene comparison using microarray analyses: comparison of replicon-expressing cell lines (Huh7/Rep-1b-Yeo and Huh7/Rep-2a-Yeo) and *cured* cells (Cured-1b/Huh7 and Cured-2a/Huh7) was intended to identify genes that are affected by HCV replication, and comparison of parental Huh7 cells and *cured* cell lines was intended to identify

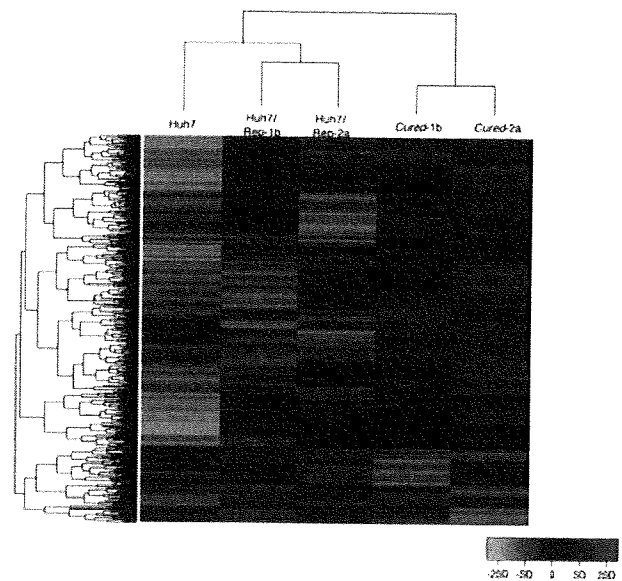


Fig. 3 Hierarchical clustering of gene expression profiles obtained from the 1b and 2a Yeo-replicon expressing cells, cured cells and Huh7. The 1,870 probe sets that changed expression more than 1.2-fold in either Huh7 versus *cured* or *cured* versus replicon were selected. Dendrograms show the classification determined by hierarchical clustering analysis. *Red* and *green* colors indicate relative overexpression and underexpression, respectively

genes that are essential for a high level of HCV replication in cultured cells.

Hierarchical clustering gene expression profiles in naïve, replicon-expressing and cured cells

Datasets from the microarrays were normalized using the robust multi-array average (RMA) method, and differentially expressed genes were extracted in replicon cells, *cured* cells and naïve Huh7 cells. Gene expression profiles were well correlated each other between duplicate microarray data from the same cell line with the Pearson's correlation coefficients (R^2) of greater than 0.975 (see Supplementary Fig. 1). In this analysis, 1,870 probe sets showed differences in expression levels of more than 1.2-fold under $\delta < 0.1$ in either Huh7 versus *cured* (1,516 probe sets) or *cured* versus replicon (372 probe sets). A hierarchical clustering analysis showed that the gene-expression profiles of each cell group constituted clear clusters, Huh7/Rep-2a and Huh7/Rep-1b, Cured-2a and Cured-1b, and Huh7 cells (Fig. 3). Among genes whose expression differed significantly between replicon-expressing cells and *cured* cells, 15 showed changes of more than two-fold (Table 1). These included cell cycle- or cell growth-related genes (nuclear protein 1, growth differentiation factor 15, urothelial cancer associated 1, inhibin and tubulin), oncogene (Ras-related GTP binding D) and interferon-related gene (IFIM3). On the other hand, 37

Table 1 Microarray analysis: genes for which the expression changed more than two-fold in Rep-1b/Huh7 and Rep-2a/Huh7 cells compared to their *cured* cells

Probe set	Title	Rep1b/cured1b		Rep2a/cured2a	
		Fold change	Q-value	Fold change	Q-value
209230_s_at	Nuclear protein 1	5.41	0.00	13.78	7.44
221523_s_at	Ras-related GTP binding D	3.82	0.00	2.32	24.60
221524_s_at	Ras-related GTP binding D	3.17	0.00	2.40	17.08
205923_at	Reelin	3.14	0.00	2.70	12.42
200924_s_at	Hypothetical protein LOC442497/solute carrier family 3 (activators of dibasic and neutral amino acid transport), member 2	2.84	0.00	2.63	0.69
221577_x_at	Growth differentiation factor 15	2.62	0.00	3.16	0.00
233030_at	Patatin-like phospholipase domain containing 3	2.07	0.00	2.31	3.16
201471_s_at	Sequestosome 1	2.52	0.81	2.10	2.45
227919_at	Urothelial cancer associated 1	5.09	0.90	2.90	54.18
207076_s_at	Argininosuccinate synthetase 1	2.99	0.90	2.22	61.28
205749_at	Cytochrome P450, family 1, subfamily A, polypeptide 1	2.69	0.90	2.63	4.55
217127_at	Cystathionase (cystathionine gamma-lyase)	2.32	3.05	2.38	6.54
210587_at	Inhibin, beta E	2.51	4.25	3.89	2.45
214023_x_at	Tubulin, beta 2B	2.41	4.25	4.31	54.18
212203_x_at	Interferon induced transmembrane protein 3 (1-8U)	2.34	5.75	2.09	54.18

genes were up-regulated by more than two-fold between *cured* and naïve cells (Table 2), which included genes such as chemokine (CCL14), solute carrier family and metallothionein family.

Pathway process analyses and hierarchical clustering of genes in each functional category

Using the KEGG Pathway database, we analyzed pathway processes that were altered between replicon-expressing cells and *cured* cells as well as between *cured* cells and Huh7 cells (Supplementary Tables 2, 3). Comparison of the pathway processes between replicon-expressing and *cured* cells identified six pathways that showed differences of $FDR < 0.3$, including pathways related to MAPK ($P = 4.0 \times 10^{-4}$, FDR 0.08), biosynthesis of steroids ($P = 4.21 \times 10^{-3}$, FDR 0.21) and TGF-beta ($P = 8.4 \times 10^{-3}$, FDR 0.29) (KEGG Pathway maps for each significant pathway are shown in Supplementary Fig. 2A–F). Comparison of the pathway processes between *cured* and naïve Huh7 cells identified 11 significant pathways (KEGG Pathway maps for each significant pathway are shown in Fig. 5 and Supplementary Fig. 3A–J). These included pathways that were related to TGF-beta ($P = 8.42 \times 10^{-3}$), cell cycle ($P = 9.0 \times 10^{-3}$) and sphingolipid metabolism ($P = 1.32 \times 10^{-2}$). Interestingly, there were significant changes in the biosynthesis of steroids ($P = 1.75 \times 10^{-4}$) between *cured* and naïve Huh7 cells. These results suggested that several lipid metabolism processes were substantially associated with efficient HCV replication in host cells.

Hierarchical clustering analyses of representative genes included in functional pathway categories

Based on pathway process analyses using the KEGG database, we performed hierarchical clustering analyses of each functional subset of genes (fold change > 1.2 , Fig. 4a–c). The cell cycle, cholesterol biosynthesis and sphingolipid metabolism-related genes demonstrated clear clusters in replicon cells, *cured* cell and parental Huh7, respectively. In particular, cholesterol biosynthesis-related genes were activated in replicon cells and *cured* cells.

Mapping between pathway information and gene expression data

Knowing that cholesterol metabolism pathway was changed substantially in *cured* cells, we performed graphical mapping of the related genes to the KEGG Pathway map database (Fig. 5). Similar to the pathway analyses, cholesterol biosynthesis related genes, which are involved in the mevalonate pathway or sterol biosynthesis, were clearly activated in *cured* cells compared to naïve Huh7 (Fig. 5).

To verify the microarray results, we performed real-time RT-PCR of cholesterol biosynthesis-related genes including HMGCR, SQLE, NSDHL, CYP51A1, TM7SF2 and EBP. All the genes were upregulated in replicon-expressing and *cured* cells compared to the naïve Huh7 cells (Fig. 6). These results were consistent with the microarray data.

Table 2 Microarray analysis: genes for which the expression changed more than two-fold in *cured-1b* and *cured-2a* cells compared to Huh7

Probe set	Title	Cured1b/Huh7		Cured2a/Huh7	
		Fold change	Q-value	Fold change	Q-value
210390_s_at	Chemokine (C–C motif) ligand 14/15	4.49	0.00	2.56	0.00
221168_at	PR domain containing 13	2.38	0.00	2.15	0.00
1553995_a_at	5'-nucleotidase, ecto (CD73)	2.15	0.00	3.64	0.36
204897_at	Prostaglandin E receptor 4 (subtype EP4)	2.07	2.40	2.19	0.36
214522_x_at	Histone cluster 1, H2ad/H3d	3.01	4.12	2.98	0.46
214472_at	Histone cluster 1, H2ad/H3a-j	3.36	5.08	3.53	0.46
218280_x_at	Histone cluster 2, H2aa3/H2aa4	4.65	5.20	5.17	0.61
232035_at	Histone cluster 1, H4a-f, H4 h-l/histone cluster 2, H4a-b/histone cluster 4, H4	5.56	6.51	5.37	0.95
214455_at	Histone cluster 1, H2bc, H2be, H2bf, H2bg, H2bi	4.72	6.51	2.68	0.61
202708_s_at	Histone cluster 2, H2be	4.48	6.51	5.31	0.95
214290_s_at	Histone cluster 2, H2aa3/H2aa4	4.06	6.51	2.98	2.08
209398_at	Histone cluster 1, H1c	3.40	6.51	3.60	2.08
230795_at	–	2.91	6.51	4.51	0.95
1553994_at	5'-nucleotidase, ecto (CD73)	2.29	6.51	2.31	3.34
208180_s_at	Histone cluster 1, H4a-f, H4 h-l/histone cluster 2, H4a, H4b/histone cluster 4, H4	6.27	7.65	3.40	1.46
215779_s_at	Histone cluster 1, H2bc, H2be, H2bf, H2bg, H2bi	3.53	7.65	5.86	1.46
206110_at	–	3.82	9.12	10.68	0.00
206535_at	Solute carrier family 2 (facilitated glucose transporter), member 2	3.58	9.12	2.84	5.02
213880_at	Leucine-rich repeat-containing G protein-coupled receptor 5	2.81	9.12	3.02	5.02
210387_at	Histone cluster 1, H2bc, H2be, H2bf, H2bg, H2bi	3.24	10.68	2.28	11.66
203044_at	Chondroitin sulfate synthase 1	2.36	11.85	2.67	2.08
207102_at	Aldo-keto reductase family 1, member D1 (delta 4-3-ketosteroid-5-beta-reductase)	2.14	13.35	5.58	0.36
219596_at	THAP domain containing 10	2.20	16.73	3.32	2.08
217997_at	Pleckstrin homology-like domain, family A, member 1	2.15	23.48	3.01	3.34
217996_at	Pleckstrin homology-like domain, family A, member 1	2.12	23.48	2.21	11.66
217165_x_at	Metallothionein 1F	3.36	29.61	3.25	11.66
213629_x_at	Metallothionein 1F	3.13	29.61	3.70	11.66
210524_x_at	–	2.39	29.61	2.46	17.81
206143_at	Solute carrier family 26, member 3	2.35	29.61	2.49	17.81
212859_x_at	Metallothionein 1E	3.46	35.93	4.07	11.66
208581_x_at	Metallothionein 1X	3.31	35.93	3.52	17.81
204326_x_at	Metallothionein 1X	3.24	35.93	3.49	17.81
211456_x_at	Metallothionein 1 pseudogene 2	3.19	35.93	3.71	17.81
206461_x_at	Metallothionein 1H	3.09	35.93	3.49	17.81
216336_x_at	Metallothionein 1E, 1H, 1 M/metallothionein 1 pseudogene 2	3.02	35.93	3.27	17.81
212185_x_at	Metallothionein 2A	2.92	35.93	2.85	17.81
204745_x_at	Metallothionein 1G	2.73	35.93	3.31	17.81

Detection of intracellular lipid droplets in naïve, replicon-expressing and cured cells

Because several lipid-related pathways were extracted (Supplementary Tables 2 and 3), we examined phenotypes of the cell lines featuring different lipid metabolism

gene expression profiles by carrying out detection of cellular lipid droplets (Fig. 8a, b). The cells were stained by Oil red O or BODIPY493/503, dye solutions specific for neutral lipids. We found a large number of lipid droplets in the cytoplasm of each Huh7 cell line. The number of lipid droplets obviously was increased more in

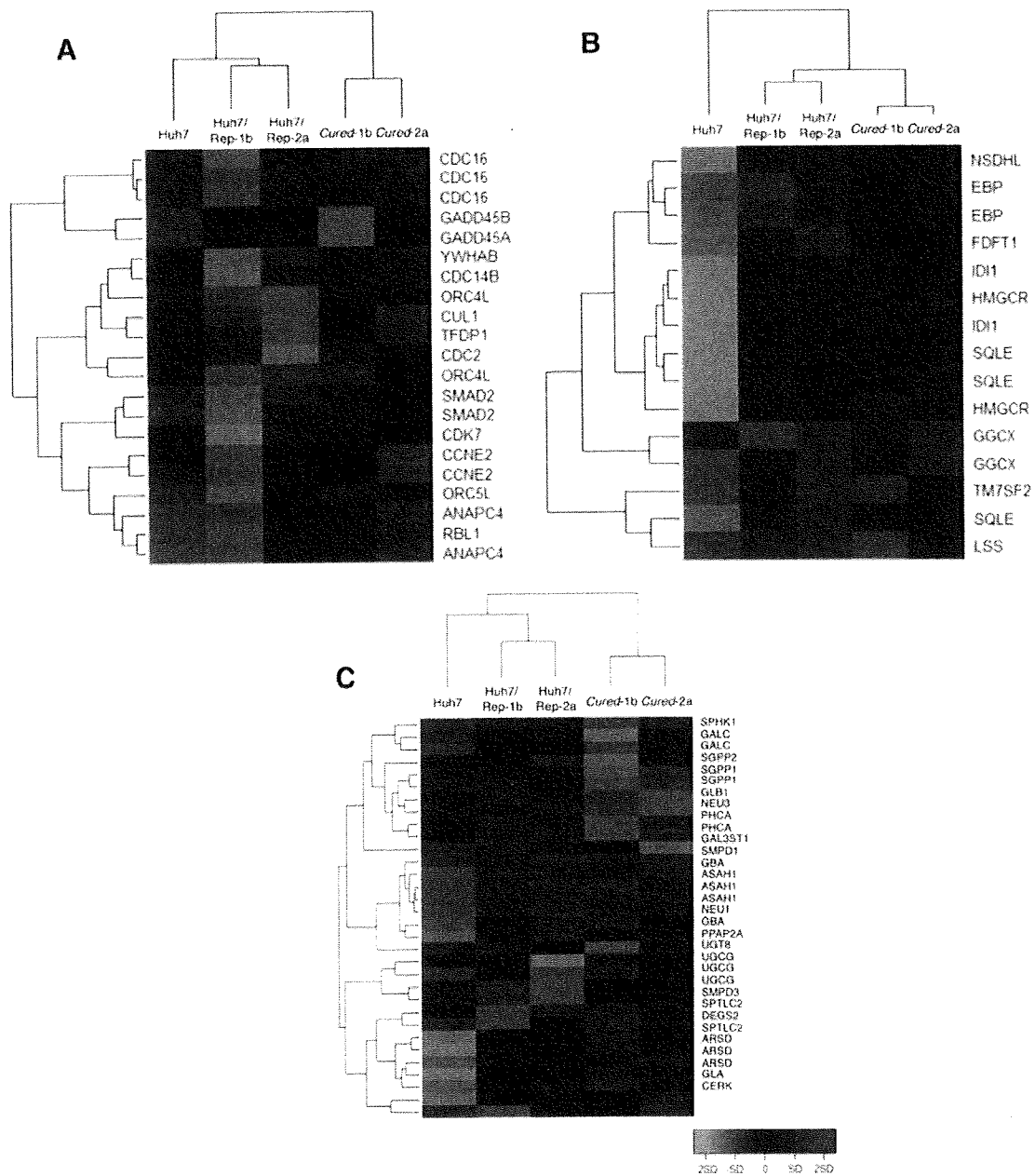


Fig. 4 Hierarchical clustering of representative genes included in each KEGG Pathway map. **a** Cell cycle, **b** cholesterol biosynthesis, **c** sphingolipid metabolism. Dendrograms shows the classification

determined by hierarchical clustering analysis. *Red and green colors* indicate relative overexpression and underexpression, respectively

the two replicon-expressing cells and the *cured* cells than in the parental Huh7 cells. Lipid and HCV-NS5A double staining showed an increase in lipid droplets in cells that expressed HCV proteins (Fig. 8b). Analyses of the KEGG fatty acid metabolism pathway showed that a substantial number of the genes of these pathways were up-regulated in the *cured* cells compared to the naïve cells, although these could not reach statistical significance (Fig. 7).

Effects of hepatitis C virus replication by PPAR-alpha and gamma agonists

To assess the effects of lipid metabolic status on the intracellular replication of the HCV genome, Huh7/Rep-Feo cells were cultured with various concentrations of several PPAR-alpha agonists (clofibrate, fenofibrate and bezafibrate) and gamma agonists (pioglitazone and troglitazone) (Fig. 9). The luciferase activities of the Huh7/

BIOSYNTHESIS OF STEROIDS

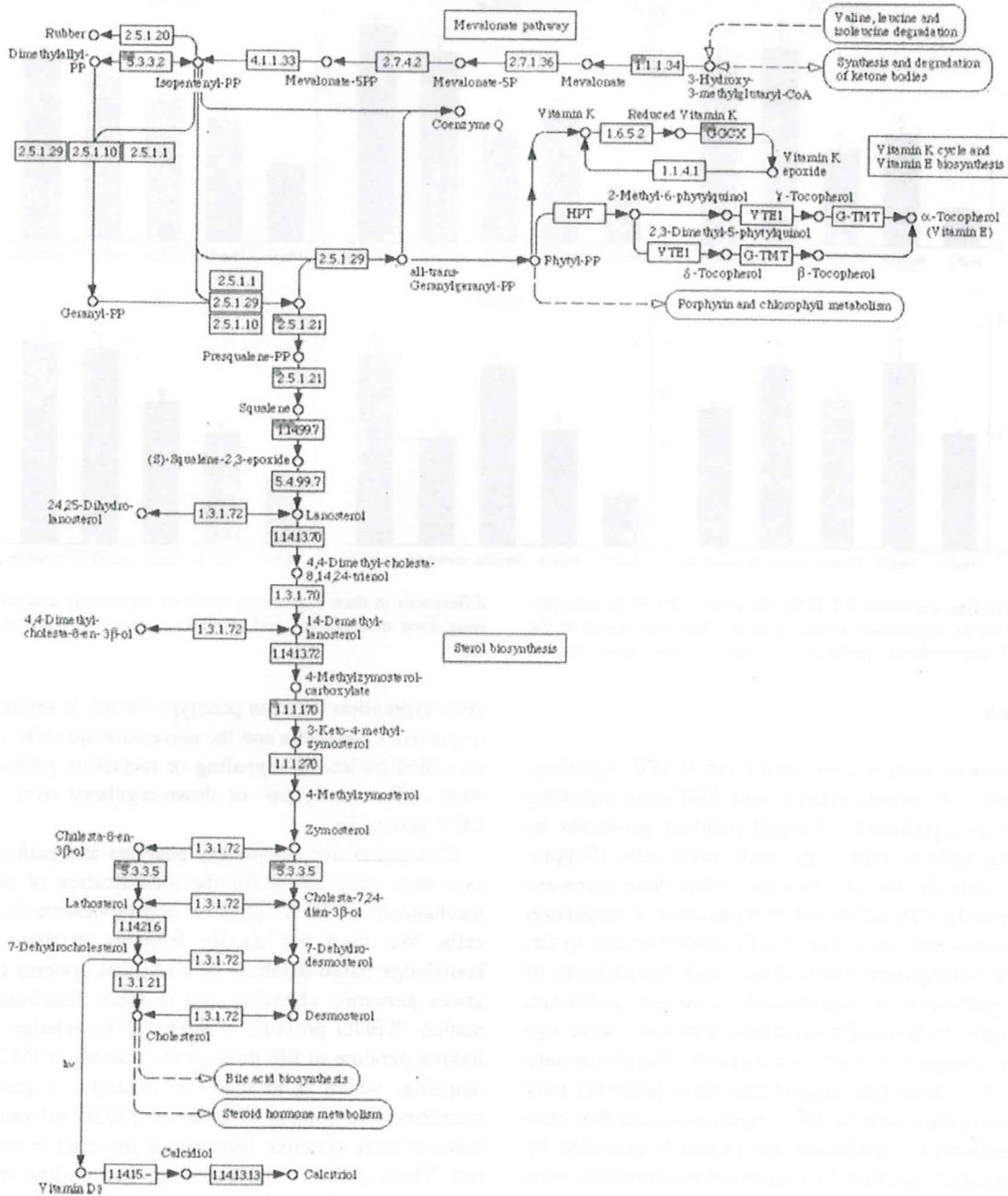


Fig. 5 KEGG Pathway map and array data (biosynthesis of steroids). Gene expression changes were mapped on the pathways. Each circle within a box represents the corresponding probe set on Human Genome U133 Plus 2.0 array because multiple probe sets are sometimes designed for a single gene. Red circles indicate overexpressed genes in cured cells compared to parental Huh7 cells. The

dotted numerical code in each box represents the Enzyme Commission (EC) number based on the recommendations of the Nomenclature Committee of the International Union of Biochemistry and Molecular Biology (IUBMB). Correspondence between the genes that were examined in the microarray analyses and enzymes that are presented in Fig. 5 is shown in Supplementary Table 4

Rep-Feo cells showed that the replication of the HCV replicon was suppressed by clofibrate and fenofibrate in a dose-dependent manner, whereas pioglitazone and troglitazone elevated expression levels of replicon. The MTS

assay did not show any effect on cell viability or replication. These results suggest that the decrease or increase in HCV replication is due to specific effects of PPAR-alpha or gamma agonists on HCV replication.

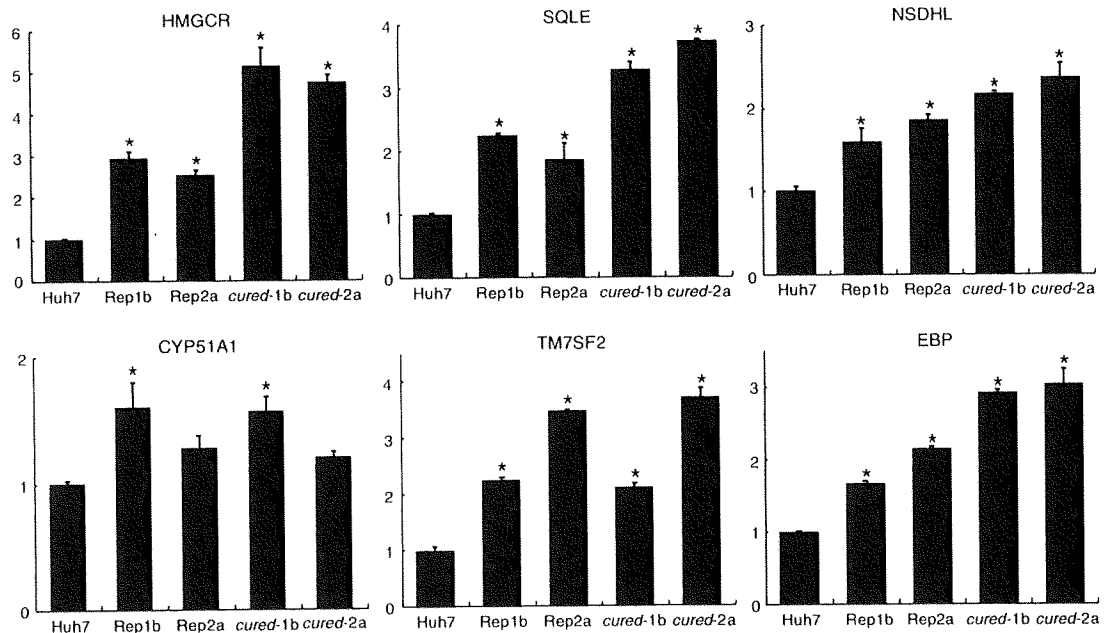


Fig. 6 Real-time detection RT-PCR. Real-time RT-PCR was performed to verify expression levels of genes that were listed in the cholesterol biosynthesis pathway in Fig. 4c and that showed

differences in their expression levels by microarray analyses. Assays were done in triplicate, and *asterisks* indicate *P*-values of less than 0.05

Discussion

In our present analyses, we identified MAPK signaling, biosynthesis of steroid related and TGF-beta signaling pathways as significantly changed pathway processes by comparing replicon-expressing and *cured* cells (Supplementary Table 2). The results suggest that these pathways were primarily affected by HCV replication. Comparison of *cured* cells and naïve Huh7 cells identified cell cycle, TGF-beta, sphingolipid metabolism, and biosynthesis of steroids pathways as significantly changed pathways. Interestingly, cholesterol biosynthesis pathways were significantly changed in both comparisons (Supplementary Tables 2, 3). These data suggest that these pathways may positively regulate cellular HCV replication and that cholesterol biosynthesis pathways are primarily activated by HCV replication and may be essential for continuous virus replication.

There are several studies that report gene expression changes in replicon-expressing Huh7 cells as compared with the naïve cells [30–32]. In those studies, however, the changes in gene expression do not only reflect the effect of intracellular HCV replication, but also reflect alteration of host cell clonalities. Indeed, there are inconsistencies among studies. Use of the *cured* Huh7 cells can minimize the effect of cellular clonal changes because such Huh7 subclones have already been selected through HCV replicon transduction, drug-resistance selection and subsequent HCV elimination [33]. In our study, we have compared

gene expression between genotype 1b and 2a replicon cells, respective *cured* cells and the naïve parental cells, and have identified molecular signaling or metabolic pathways that were differentially up- or down-regulated over different HCV genotypes.

Comprehensive microarray analyses and pathway analyses were very useful for the identification of molecular mechanisms of HCV infection and replication in the host cells. We used the KEGG Pathway database [28], a knowledge-based database of biological systems that integrates genomic, chemical and systemic functional information. KEGG provides a reference knowledge base for linking genome to life through the process of PATHWAY mapping, which is to map, for example, a genomic or transcriptomic content of genes to KEGG reference pathways to infer systemic behavior of the cells or the organism. These pathway databases are free on-line resources. Using these analyses, the close relation between cholesterol metabolism and HCV replication was demonstrated. Moreover, in relation to this, when we examined the pathways of other lipid metabolism, it was shown that fatty acid biosynthesis metabolism-related pathways were significantly changed in *cured* cells, and indeed we found a large number of lipid droplets in the cytosol of replicon cells and *cured* cells.

The HCV-JFH1 strain is the basis of a robustly replicating cell culture system reported recently [5]. We have performed comprehensive gene expression analyses using the HCV-JFH1 and the *cured* Huh7.5.1 cell line [6]. The

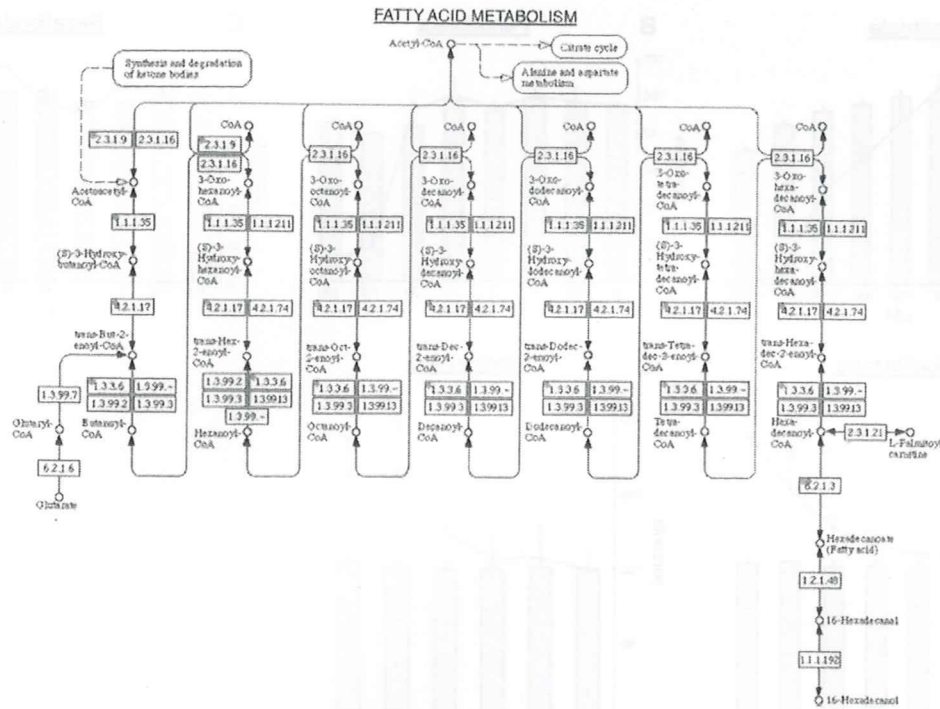
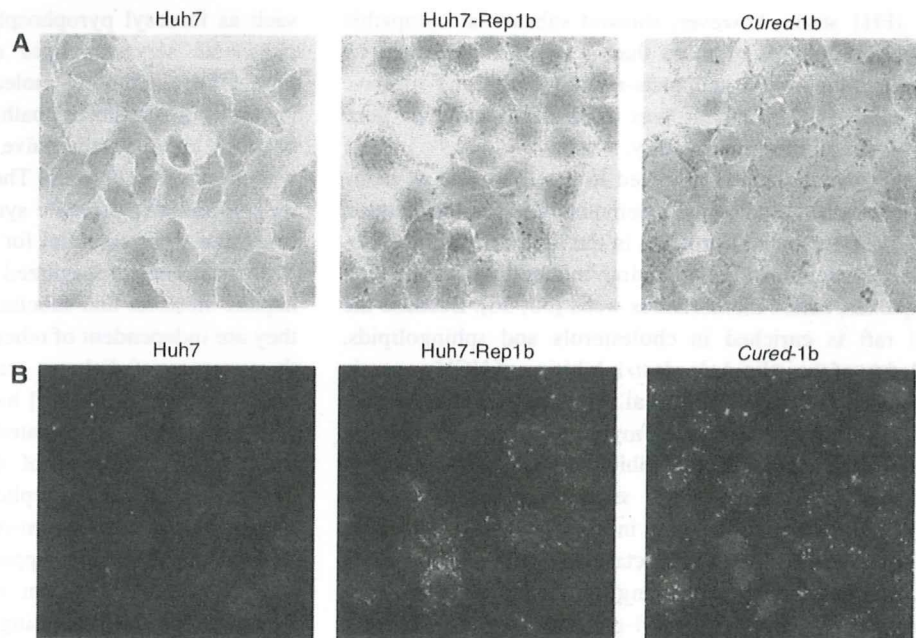


Fig. 7 KEGG Pathway map and array data (fatty acid metabolism). Gene expression changes were mapped on the pathways. Each circle within a box represents the corresponding probe set on Human Genome U133 Plus 2.0 array because multiple probe sets are sometimes designed for a single gene. Red circles indicate overexpressed genes in

cured cells compared to parental Huh7 cells. The dotted numerical code in each box represents the Enzyme Commission (EC) number. Correspondence between the genes that were examined in the microarray analyses and enzymes that are presented in Fig. 7 are shown in Supplementary Table 4

Fig. 8 Detection of intracellular lipid droplets and HCV NS protein. **a** Huh7 cells, replicon cells and cured cells were fixed and stained with Oil red O and Mayer’s hematoxylin. Intracellular lipid droplets were detected as red spheres in the cells. Nuclei are stained in blue. **b** Rep1b/Huh7 cells were labeled with antibodies against NS5A (red). Lipid droplets and nuclei were stained with BODIPY493/503 (green) and DAPI (blue), respectively



KEGG Pathway analyses have identified several significantly affected pathways that are involved in the cell cycle, TGF-beta signaling, PPAR signaling and sterol

biosynthesis. These findings are consistent with our present results using the HCV subgenomic replicon (see the Supplementary Table 5; Supplementary Figs. 4, 5).

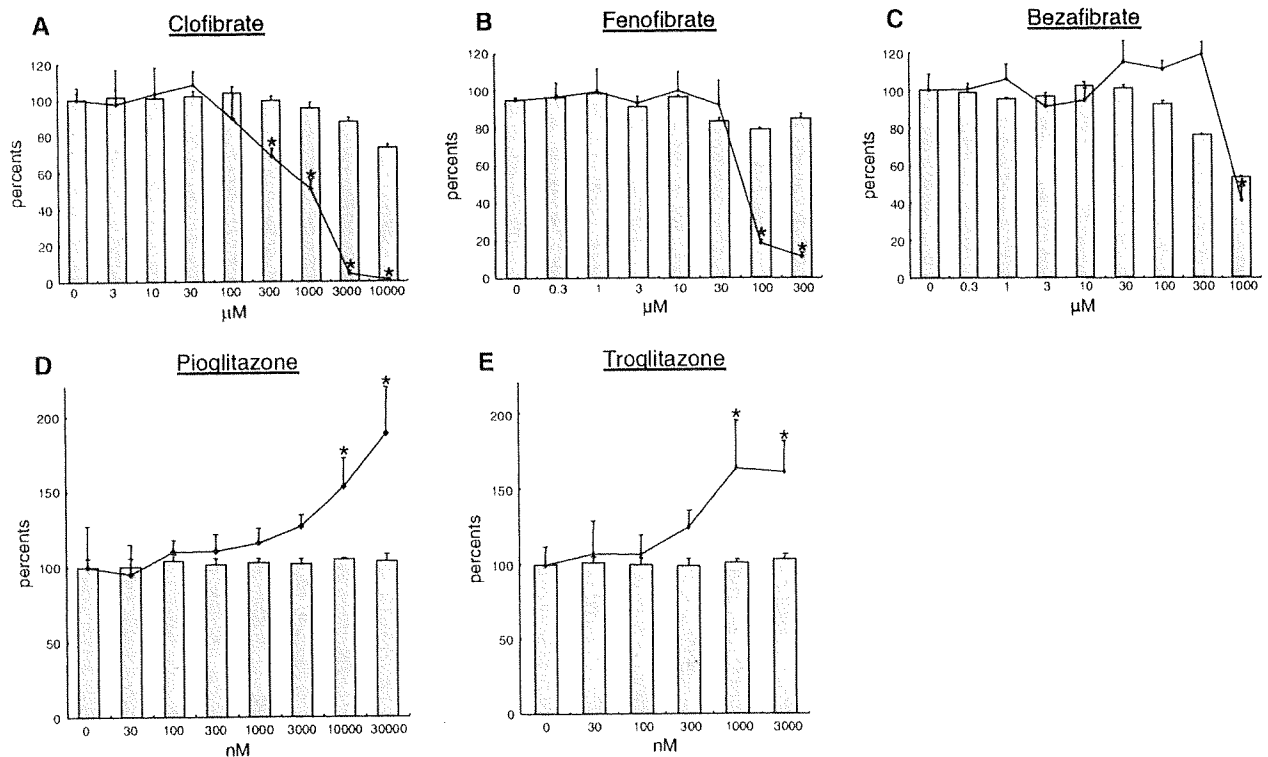


Fig. 9 Results of secondary screening with PPAR- α and - γ agonists. Luciferase activity for HCV replication levels is shown as a percentage of the control. Cell viability is also shown as percentage of

the control. Each bar represents the average of quadruplicate data points with standard deviation represented as the error bar. Asterisks denotes a significant difference from the control of at least $P < 0.05$

The JFH1 strain, however, showed substantial cytopathic effects on cultures of more than 5 days accompanied by overall induction of apoptosis-related genes and massive cell death [34]. Thus, it was difficult to conduct gene expression studies consistently.

Lipid metabolism is involved in the life cycle of many viruses. Recent studies have demonstrated the localization of HCV nonstructural proteins in the lipid raft in the endoplasmic reticulum (ER) forming intracellular replication complexes, called membranous webs [35, 36]. Because the lipid raft is enriched in cholesterol and sphingolipids, depletion of these lipids leads to inhibition of HCV genomic replication [19]. Amemiya et al. [37] reported that another serine palmitoyltransferase, myriocin, depleted cellular sphingomyelin contents and inhibited HCV replication.

It has been reported that statins efficiently suppress HCV replication in vitro and in vivo [38–40]. Statins are inhibitors of HMG-CoA reductase and shut down cholesterol biosynthesis by preventing the formation of mevalonate from 3-hydroxy-3-methyl-glutaryl CoA. As we have shown in the results, all enzymes in the cholesterol synthesis pathway were upregulated in the replicon-expressing and the cured Huh7 cells. In addition to lowering intracellular levels of sterols, statins also reduce levels of isoprenoids, which are derived from mevalonate. Isoprenoids

such as farnesyl pyrophosphate and geranylgeranyl pyrophosphate serve as lipid attachments for a variety of intracellular signaling molecules. In our results, the cholesterol biosynthesis pathway was also upregulated between cured versus naïve cell lines as well as replicon versus cured cell lines. These results suggest that HCV replication may promote synthesis of lipids including steroids that were essential for the viral efficient replication.

It has been recognized that HCV infection causes hepatic steatosis and subclinical insulin resistance and that they are independent of other risk factors such as obesity or the presence of diabetes mellitus. Similarly, in HCV cell cultures, Yang et al. [41] have reported that cellular fatty acid synthase is upregulated in HCV-infected Huh7 cells and specific inhibition of the enzymatic activity caused suppression of HCV replication. In the present study, although lipid metabolism-related genes were upregulated in cured cells, which supports efficient HCV replication, there was not significant change in lipid-related genes between replicon-expressing as compared with cured cells (Fig. 7). These results suggest that HCV subgenomic replication does not cause steatosis as it did in full-length HCV cell culture [41]. These discrepancies might be due to the absence of the presence of HCV structural genes including core and envelope proteins.

We have shown an increase in lipid droplets in HCV replicon-positive cells and their cured cell lines as a phenotype of the gene expression profiles (Fig. 8). On the other hand, ACOX1, a rate-limiting enzyme of peroxisomal beta-oxidation, was higher in cured cells than parental Huh7 cells (Fig. 7) [42]. We have shown preliminarily that cellular SREBP1 (sterol regulatory element-binding protein 1), which regulates a set of triglyceride synthesis enzymes en bloc, is upregulated in HCV replicon-positive cell lines. These discrepancies might be due to more proficient activation of SREBP1-induced fatty acid biosynthesis pathways. Collectively, our results suggest that the overall fatty acid synthesis pathway, not only fatty acid synthase, is activated by upregulation of a set of responsible enzymes.

We have investigated effects of PPAR agonists to HCV replication. PPAR-alpha agonists, clofibrate and fenofibrate suppressed HCV replication (Fig. 9). PPAR-alpha, not PPAR-gamma, is expressed in hepatocytes, recognizes cellular free fatty acids and leukotriene B4 as a specific ligands, and mediates oxidative degradation of triglyceride and depletion of intracellular fat droplets [43, 44]. These properties of PPAR-alpha agonists suggest that the level of HCV replication is affected by the increased production of fatty acids, but not by the overexpression of their related enzymes. PPAR-gamma agonists, in contrast, amplified HCV replication. Because PPAR-gamma is a regulator of fatty acid metabolism in peripheral tissue and is not expressed in the hepatocytes or in Huh7 cells (data not shown), it is possible that the effects of the PPAR-gamma agonists on HCV replication may be through its pleiotropic side effects such as p38 MAPK activation [45]. Very recently, it has been reported that HCV-NS5A proteins induce expression of PPARgamma [46].

In conclusion, comprehensive gene expression and pathway analyses were useful to study molecular pathways that were involved in HCV pathogenesis and to identify host factors for HCV replication that could constitute antiviral targets.

Acknowledgment This study was supported by grants from Ministry of Education, Culture, Sports, Science and Technology-Japan, the Japan Society for the Promotion of Science, Ministry of Health, Labour and Welfare-Japan, Japan Health Sciences Foundation, and National Institute of Biomedical Innovation.

References

- Alter MJ. Epidemiology of hepatitis C. *Hepatology*. 1997;26:62S–5S.
- Hadziyannis SJ, Sette H Jr, Morgan TR, Balan V, Diago M, Marcellin P, et al. Peginterferon-alpha2a and ribavirin combination therapy in chronic hepatitis C: a randomized study of treatment duration and ribavirin dose. *Ann Intern Med*. 2004;140:346–55.
- Sakamoto N, Watanabe M. New therapeutic approaches to hepatitis C virus. *J Gastroenterol*. 2009;44:643–9.
- Lohmann V, Korner F, Koch J, Herian U, Theilmann L, Bartenschlager R. Replication of subgenomic hepatitis C virus RNAs in a hepatoma cell line. *Science*. 1999;285:110–3.
- Wakita T, Pietschmann T, Kato T, Date T, Miyamoto M, Zhao Z, et al. Production of infectious hepatitis C virus in tissue culture from a cloned viral genome. *Nat Med*. 2005;11:791–6.
- Zhong J, Gastaminza P, Cheng G, Kapadia S, Kato T, Burton DR, et al. Robust hepatitis C virus infection in vitro. *Proc Natl Acad Sci USA*. 2005;102:9294–9.
- Tai AW, Benita Y, Peng LF, Kim SS, Sakamoto N, Xavier RJ, et al. A functional genomic screen identifies cellular cofactors of hepatitis C virus replication. *Cell Host Microbe*. 2009;5:298–307.
- Itsui Y, Sakamoto N, Kurosaki M, Kanazawa N, Tanabe Y, Koyama T, et al. Expression screening of interferon-stimulated genes for antiviral activity against hepatitis C virus replication. *J Viral Hepat*. 2006;13:690–700.
- Yamashiro T, Sakamoto N, Kurosaki M, Kanazawa N, Tanabe Y, Nakagawa M, et al. Negative regulation of intracellular hepatitis C virus replication by interferon regulatory factor 3. *J Gastroenterol*. 2006;41:750–7.
- Foy E, Li K, Sumpter R Jr, Loo YM, Johnson CL, Wang C, et al. Control of antiviral defenses through hepatitis C virus disruption of retinoic acid-inducible gene-1 signaling. *Proc Natl Acad Sci USA*. 2005;102:2986–91.
- Sakamoto N, Yoshimura M, Kimura T, Toyama K, Sekine-Osajima Y, Watanabe M, et al. Bone morphogenetic protein-7 and interferon-alpha synergistically suppress hepatitis C virus replicon. *Biochem Biophys Res Commun*. 2007;357:467–73.
- Murata T, Ohshima T, Yamaji M, Hosaka M, Miyanari Y, Hijikata M, et al. Suppression of hepatitis C virus replicon by TGF-beta. *Virology*. 2005;331:407–17.
- Shimakami T, Honda M, Kusakawa T, Murata T, Shimotohno K, Kaneko S, et al. Effect of hepatitis C virus (HCV) NS5B-nucleolin interaction on HCV replication with HCV subgenomic replicon. *J Virol*. 2006;80:3332–40.
- Nakagawa M, Sakamoto N, Tanabe Y, Koyama T, Itsui Y, Takeda Y, et al. Suppression of hepatitis C virus replication by cyclosporin A is mediated by blockade of cyclophilins. *Gastroenterology*. 2005;129:1031–41.
- Tardif KD, Mori K, Siddiqui A. Hepatitis C virus subgenomic replicons induce endoplasmic reticulum stress activating an intracellular signaling pathway. *J Virol*. 2002;76:7453–9.
- Wang J, Tong W, Zhang X, Chen L, Yi Z, Pan T, et al. Hepatitis C virus non-structural protein NS5A interacts with FKBP38 and inhibits apoptosis in Huh7 hepatoma cells. *FEBS Lett*. 2006;580:4392–400.
- Choi YW, Tan YJ, Lim SG, Hong W, Goh PY. Proteomic approach identifies HSP27 as an interacting partner of the hepatitis C virus NS5A protein. *Biochem Biophys Res Commun*. 2004;318:514–9.
- Okamoto T, Nishimura Y, Ichimura T, Suzuki K, Miyamura T, Suzuki T, et al. Hepatitis C virus RNA replication is regulated by FKBP8 and Hsp90. *EMBO J*. 2006;25:5015–25.
- Sakamoto H, Okamoto K, Aoki M, Kato H, Katsume A, Ohta A, et al. Host sphingolipid biosynthesis as a target for hepatitis C virus therapy. *Nat Chem Biol*. 2005;1:333–7.
- Yokota T, Sakamoto N, Enomoto N, Tanabe Y, Miyagishi M, Maekawa S, et al. Inhibition of intracellular hepatitis C virus replication by synthetic and vector-derived small interfering RNAs. *EMBO Rep*. 2003;4:602–8.
- Tanabe Y, Sakamoto N, Enomoto N, Kurosaki M, Ueda E, Maekawa S, et al. Synergistic inhibition of intracellular hepatitis C virus replication by combination of ribavirin and interferon-alpha. *J Infect Dis*. 2004;189:1129–39.

22. Guo JT, Bichko VV, Seeger C. Effect of alpha interferon on the hepatitis C virus replicon. *J Virol*. 2001;75:8516–23.
23. Donnelly MLL, Hughes LE, Luke G, Mendoza H, ten Dam E, Gani D, et al. The 'cleavage' activities of foot-and-mouth disease virus 2A site-directed mutants and naturally occurring '2A-like' sequences. *J Gen Virol*. 2001;82:1027–41.
24. Nakagawa M, Sakamoto N, Enomoto N, Tanabe Y, Kanazawa N, Koyama T, et al. Specific inhibition of hepatitis C virus replication by cyclosporin A. *Biochem Biophys Res Commun*. 2004;313:42–7.
25. Blight KJ, McKeating JA, Rice CM. Highly permissive cell lines for subgenomic and genomic hepatitis C virus RNA replication. *J Virol*. 2002;76:13001–14.
26. Strand C, Enell J, Hedenfalk I, Ferno M. RNA quality in frozen breast cancer samples and the influence on gene expression analysis—a comparison of three evaluation methods using microcapillary electrophoresis traces. *BMC Mol Biol*. 2007;8:38.
27. Tusher VG, Tibshirani R, Chu G. Significance analysis of microarrays applied to the ionizing radiation response. *Proc Natl Acad Sci USA*. 2001;98:5116–21.
28. Kanehisa M, Araki M, Goto S, Hattori M, Hirakawa M, Itoh M, et al. KEGG for linking genomes to life and the environment. *Nucleic Acids Res*. 2008;36:D480–4.
29. Benjamini Y, Hochberg Y. Controlling the false discovery rate: a practical and powerful approach to multiple testing. *J R Stat Soc B*. 1995;57:289–300.
30. Ciccaglione AR, Marcantonio C, Tritarelli E, Tataseo P, Ferraris A, Bruni R, et al. Microarray analysis identifies a common set of cellular genes modulated by different HCV replicon clones. *BMC Genomics*. 2008;9:309.
31. Hayashi J, Stoyanova R, Seeger C. The transcriptome of HCV replicon expressing cell lines in the presence of alpha interferon. *Virology*. 2005;335:264–75.
32. Scholle F, Li K, Bodola F, Ikeda M, Luxon BA, Lemon SM. Virus–host cell interactions during hepatitis C virus RNA replication: impact of polyprotein expression on the cellular transcriptome and cell cycle association with viral RNA synthesis. *J Virol*. 2004;78:1513–24.
33. Abe K, Ikeda M, Dansako H, Naka K, Shimotohno K, Kato N. cDNA microarray analysis to compare HCV subgenomic replicon cells with their cured cells. *Virus Res*. 2005;107:73–81.
34. Sekine-Osajima Y, Sakamoto N, Nakagawa M, Itsui Y, Tasaka M, Nishimura-Sakurai Y, et al. Development of plaque assays for hepatitis C virus and isolation of mutants with enhanced cytopathogenicity and replication capacity. *Virology*. 2008;371:71–85.
35. Mottola G, Cardinali G, Ceccacci A, Trozzi C, Bartholomew L, Torrisi MR, et al. Hepatitis C virus nonstructural proteins are localized in a modified endoplasmic reticulum of cells expressing viral subgenomic replicons. *Virology*. 2002;293:31–43.
36. Gosert R, Egger D, Lohmann V, Bartenschlager R, Blum HE, Bienz K, et al. Identification of the hepatitis C virus RNA replication complex in Huh-7 cells harboring subgenomic replicons. *J Virol*. 2003;77:5487–92.
37. Amemiya F, Maekawa S, Itakura Y, Kanayama A, Takano S, Yamaguchi T, et al. Targeting lipid metabolism in the treatment of hepatitis C. *J Infect Dis*. 2008;197:361–70.
38. Ikeda M, Abe K, Yamada M, Dansako H, Naka K, Kato N. Different anti-HCV profiles of statins and their potential for combination therapy with interferon. *Hepatology*. 2006;44:117–25.
39. Kim SS, Peng LF, Lin W, Choe WH, Sakamoto N, Kato N, et al. A cell-based, high-throughput screen for small molecule regulators of hepatitis C virus replication. *Gastroenterology*. 2007;132:311–20.
40. Bader T, Fazili J, Madhoun M, Aston C, Hughes D, Rizvi S, et al. Fluvastatin inhibits hepatitis C replication in humans. *Am J Gastroenterol*. 2008;103:1383–9.
41. Yang W, Hood BL, Chadwick SL, Liu S, Watkins SC, Luo G, et al. Fatty acid synthase is up-regulated during hepatitis C virus infection and regulates hepatitis C virus entry and production. *Hepatology*. 2008;48:1396–403.
42. Li Y, Tharappel JC, Gooper S, Glenn M, Glauret HP, Spear BT. Expression of the hydrogen peroxide-generating enzyme fatty acyl CoA oxidase activates NF-kappaB. *DNA Cell Biol*. 2000;19:113–20.
43. Costet P, Legendre C, More J, Edgar A, Galtier P, Pineau T. Peroxisome proliferator-activated receptor alpha-isoform deficiency leads to progressive dyslipidemia with sexually dimorphic obesity and steatosis. *J Biol Chem*. 1998;273:29577–85.
44. Kersten S, Seydoux J, Peters JM, Gonzalez FJ, Desvergne B, Wahli W. Peroxisome proliferator-activated receptor alpha mediates the adaptive response to fasting. *J Clin Invest*. 1999;103:1489–98.
45. Schiefelbein D, Seitz O, Goren I, Dissmann JP, Schmidt H, Bachmann M, et al. Keratinocyte-derived vascular endothelial growth factor biosynthesis represents a pleiotropic side effect of peroxisome proliferator-activated receptor-gamma agonist troglitazone but not rosiglitazone and involves activation of p38 mitogen-activated protein kinase: implications for diabetes-impaired skin repair. *Mol Pharmacol*. 2008;74:952–63.
46. Kim K, Kim KH, Ha E, Park JY, Sakamoto N, Cheong J. Hepatitis C virus NS5A protein increases hepatic lipid accumulation via induction of activation and expression of PPARgamma. *FEBS Lett*. 2009;583:2720–6.
47. Kato T, Date T, Miyamoto M, Furusaka A, Tokushige K, Mizokami M, et al. Efficient replication of the genotype 2a hepatitis C virus subgenomic replicon. *Gastroenterology*. 2003;125:1808–17.

Inhibition of hepatitis C virus replication by chloroquine targeting virus-associated autophagy

Tomokazu Mizui · Shunhei Yamashina · Isei Tanida · Yoshiyuki Takei · Takashi Ueno · Naoya Sakamoto · Kenichi Ikejima · Tsuneo Kitamura · Nobuyuki Enomoto · Tatsuo Sakai · Eiki Kominami · Sumio Watanabe

Received: 28 May 2009 / Accepted: 22 August 2009 / Published online: 17 September 2009
© Springer 2009

Abstract

Background Autophagy has been reported to play a pivotal role on the replication of various RNA viruses. In this study, we investigated the role of autophagy on hepatitis C virus (HCV) RNA replication and demonstrated anti-HCV effects of an autophagic proteolysis inhibitor, chloroquine. **Methods** Induction of autophagy was evaluated following the transfection of HCV replicon to Huh-7 cells. Next, we investigated the replication of HCV subgenomic replicon in response to treatment with lysosomal protease inhibitors or pharmacological autophagy inhibitor. The effect on

HCV replication was analyzed after transfection with siRNA of ATG5, ATG7 and light-chain (LC)-3 to replicon cells. The antiviral effect of chloroquine and/or interferon- α (IFN α) was evaluated.

Results The transfection of HCV replicon increased the number of autophagosomes to about twofold over untransfected cells. Pharmacological inhibition of autophagic proteolysis significantly suppressed expression level of HCV replicon. Silencing of autophagy-related genes by siRNA transfection significantly blunted the replication of HCV replicon. Treatment of replicon cells with chloroquine

T. Mizui (✉) · S. Yamashina · K. Ikejima · T. Kitamura · S. Watanabe
Department of Gastroenterology, Juntendo University,
School of Medicine, Hongo 2-1-1, Bunkyo-ku,
Tokyo 113-8421, Japan
e-mail: don-chip@aqua.email.ne.jp

S. Yamashina
e-mail: ryou0607jp@ybb.ne.jp

K. Ikejima
e-mail: ikejima@juntendo.ac.jp

T. Kitamura
e-mail: kitamura@juntendo.ac.jp

S. Watanabe
e-mail: sumio@juntendo.ac.jp

I. Tanida
Department of Biochemistry and Cell Biology,
Laboratory of Biomembranes, National Institute
of Infectious Disease, Toyama 1-23-1, Shinjuku-ku,
Tokyo 162-8640, Japan
e-mail: tanida@nih.go.jp

Y. Takei
Department of Gastroenterology, Mie University,
Kurimamachiya-cho 1577, Tsu, Mie 514-8507, Japan
e-mail: ytakei@clin.medic.mie-u.ac.jp

T. Ueno · E. Kominami
Department of Biochemistry,
Juntendo University School of Medicine,
Hongo 2-1-1, Bunkyo-ku, Tokyo 113-8421, Japan
e-mail: upfield@juntendo.ac.jp

E. Kominami
e-mail: kominami@juntendo.ac.jp

N. Sakamoto
Department of Gastroenterology and Hepatology,
Tokyo Medical and Dental University,
Yushima 1-5-45, Bunkyo-ku, Tokyo 113-8510, Japan
e-mail: nsakamoto.gast@tmd.ac.jp

N. Enomoto
First Department of Internal Medicine,
University of Yamanashi, Kakedo 4-3-11,
Kofu-shi, Yamanashi 400-8511, Japan
e-mail: enomoto@yamanashi.ac.jp

T. Sakai
Department of Anatomy,
Juntendo University School of Medicine,
Hongo 2-1-1, Bunkyo-ku, Tokyo 113-8421, Japan
e-mail: tatsuo@juntendo.ac.jp

suppressed the replication of the HCV replicon in a dose-dependent manner. Furthermore, combination treatment of chloroquine to IFN α enhanced the antiviral effect of IFN α and prevented re-propagation of HCV replicon. Protein kinase R was activated in cells treated with IFN α but not with chloroquine. Incubation with chloroquine decreased degradation of long-lived protein leucine.

Conclusion The results of this study suggest that the replication of HCV replicon utilizes machinery involving cellular autophagic proteolysis. The therapy targeted to autophagic proteolysis by using chloroquine may provide a new therapeutic option against chronic hepatitis C.

Keywords Autophagy · Autophagosome · HCV replicon · Chloroquine

Introduction

The genome of HCV, a member of the family Flaviviridae, consists of a positive-sense single-stranded RNA. Peg-interferon/ribavirin combination therapy, which is the most effective therapy against HCV infection, is effective in around 50% for genotype 1 and 80% for genotypes 2 and 3 [1–3], however, many people cannot tolerate the serious side effects and are resistant to Peg-interferon/ribavirin combination therapy. Difficulties in eradicating HCV are attributable to the limited number of treatment options against HCV [4, 5]. Therefore, the search for novel therapeutic agents remains a strong aspiration.

Autophagy is an evolutionarily conserved cellular pathway in which the cytoplasm and organelles are engulfed within double-membraned vesicles, known as autophagosomes. While cellular autophagy is thought to be in preparation for the turnover and recycling of cellular constituents [6–8], this process has been proposed as a mechanism of virus replication complex formation in positive-stranded RNA viruses including poliovirus, equine arteritis virus and coronavirus [9–12]. In these viruses, the replication complexes consist of double membrane vesicles in the cytoplasm, suggestive of an autophagosome origin [9, 12]. Recently, it was reported that transfection of HCV replicon induced autophagy [11]. Additionally, Sir et al. [13] demonstrated that the suppression of autophagy inhibited the replication of HCV. These findings suggested that the autophagy plays a pivotal role in HCV replication.

Chloroquine, which is widely used for the treatment of malaria, is a well-established inhibitor of autophagic proteolysis which acts by inhibiting acidification of lysosomes and endosomes [14]. It has been reported that chloroquine exerts direct antiviral effects on several RNA viruses including coronaviruses, flaviviruses and human immunodeficiency virus (HIV) [8, 15–17]. Moreover, clinical

studies have demonstrated the safety, tolerability, and efficacy of chloroquine in the antiviral treatment of HIV infection [18, 19]. Here, we have demonstrated that autophagic proteolysis plays a pivotal role on HCV replication, moreover, the inhibition of autophagic proteolytic pathways can constitute an effective new therapeutic target against HCV.

Materials and methods

Cell culture and treatment

Huh-7 cells were stably transfected with HCV replicon expressing chimeric protein of firefly luciferase and neomycin phosphotransferase [20, 21]. They were cultured in Dulbecco's modified essential medium (DMEM) (Sigma, St. Louis, MO) supplemented with 10% foetal bovine serum (FBS) at 37°C under 5% CO₂. To maintain cell lines carrying the HCV replicon, G418 (Wako, Osaka, Japan) was added to the medium at a final concentration 500 μ g/ml.

Luciferase assay

Luciferase activities were quantified to evaluate the replication of HCV replicon by a luminometer (Lumat LB9507; Berthold, Germany) using a Bright-Glo Luciferase Assay System (Promega, Madison, WI). Assays were performed in triplicate, and the results were expressed as mean \pm SD as percents of controls.

Cell viability assay

The viability of cells was assessed by WST-1 assay. Cells were cultured in 96-well plates at 5×10^3 /well for 24 h, and then treated with 3-methyladenine [22] (10 mM), mixture of E64d (1 μ g/ml) and pepstatin A [23] (1 μ g/ml), and chloroquine (10^{-6} – 10^{-3} M) for 18 h. Cell proliferation reagent WST-1 (Roche, Swiss) was added to each well, and the cells were incubated for another 1 h at 37°C. The absorbance was measured against a background control by microplates reader (SPECTRA max 340PC, Molecular Devices, Sunnyvale, CA) at 450 nm. The reference wavelength was 650 nm.

Inhibition of autophagy and replication of HCV replicon

Cells were treated with 3-methyladenine (10 mM) or mixture of E64d (1 μ g/ml) and pepstatin A (1 μ g/ml), chloroquine (10^{-7} – 10^{-3} M), interferon (IFN) α (100 U/ml) for 18 h, the levels of replication of HCV replicon were assessed by luciferase assay. Moreover, cells were cultured

with chloroquine (10^{-5} M) and/or IFN α (100 U/ml) for 7 days, then continued to incubate without drugs for another 21 days. Replication levels of HCV replicon were determined by luciferase assay at 7th and 21st days from cessation of drugs.

Identification of autophagosomes

Naïve Huh7 cells, Huh7/Rep-Feo cells, and Huh7/Rep-Feo treated with IFN α for 14 days were seeded on 30 mm dishes and incubated for 48 h. In addition, Huh7/Rep-Feo cells were treated with chloroquine (10^{-5} M) for 18 h. Cells were prefixed with 2% glutaraldehyde, post-fixed with 1% osmic acid, dehydrated in graded ethanol, embedded in resin, and cut into sections on an ultramicrotome. The cells were analyzed by a transmission electron microscope (Hitachi H7100, Japan). The number of autolysosomes in $100 \mu\text{m}^2$ of cytoplasm was counted by using transmission electron microscopy.

Small interfering RNA knockdown of ATG5, 7, LC-3

A combination of four chemically synthesized siRNA duplex molecules targeted to the human ATG5, 7, LC-3 α , LC-3 β mRNA sequence (Dharmacon, Lafayette, CO) was transiently transfected (final concentration 50 nM) into Huh7/Rep-Feo cells using a transfection reagent (Dharmacon, Lafayette, CO). siRNA targeted to enhanced green fluorescence protein was used as a control. Forty-eight hours after transfection, levels of HCV replication were analyzed by luciferase assay.

Western blot analysis

Twenty-five micrograms of total cell lysates were subjected to SDS/PAGE on a 10% gradient gel and electrophoretically transferred onto polyvinylidene fluoride membranes. After blocking with 5% non-fat dry milk in Tris-buffered saline, membranes were incubated with primary rabbit monoclonal antibody against Phospho-protein kinase R (P-PKR) (Cell Signaling Technology, Danvers, MA) or light-chain 3 (LC3), followed by a secondary horseradish peroxidase (HRP)-conjugated anti-rabbit IgG antibody (Cell Signaling Technology, Danvers, MA). Subsequently, specific bands were visualized using ECL detection kit (Amersham Pharmacia Biotech, Midland, ON, Canada).

Protein degradation assay

Long lived protein is mainly degraded by autophagy [24]. Cells were incubated with Williams' E/10% FBS

containing $0.5 \mu\text{Ci/ml}$ [^{14}C]leucine for 24 h to label long-lived proteins. Cells were washed with Williams' E/10% FBS containing 10^{-5} M of unlabeled leucine and incubated with the medium for 2 h to allow degradation of short-lived proteins and minimize the incorporation of labeled leucine. The cells were then washed with phosphate-buffered saline (PBS) and incubated at 37°C with Williams' E/10% FBS in the presence or absence of chloroquine (10^{-5} M). After 4 h, aliquots of the medium were taken and a one-tenth volume of 100% trichloroacetic acid was added to each aliquot. The mixtures were centrifuged at $12,000g$ for 5 min, and the acid-soluble radioactivity was determined using a liquid scintillation counter. At the end of the experiment, the cultures were washed twice with PBS, and 1 ml of cold trichloroacetic acid was added to fix the cell proteins. The fixed cell monolayers were washed with trichloroacetic acid and dissolved in 1 ml of 1 N NaOH at 37°C . Radioactivity in an aliquot of 1 N NaOH was determined by liquid scintillation counting. The percentage of protein degradation was calculated according to published procedures [25].

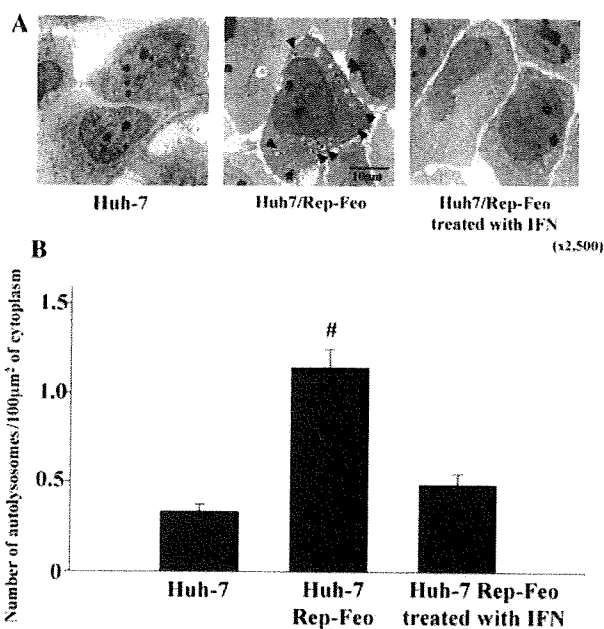
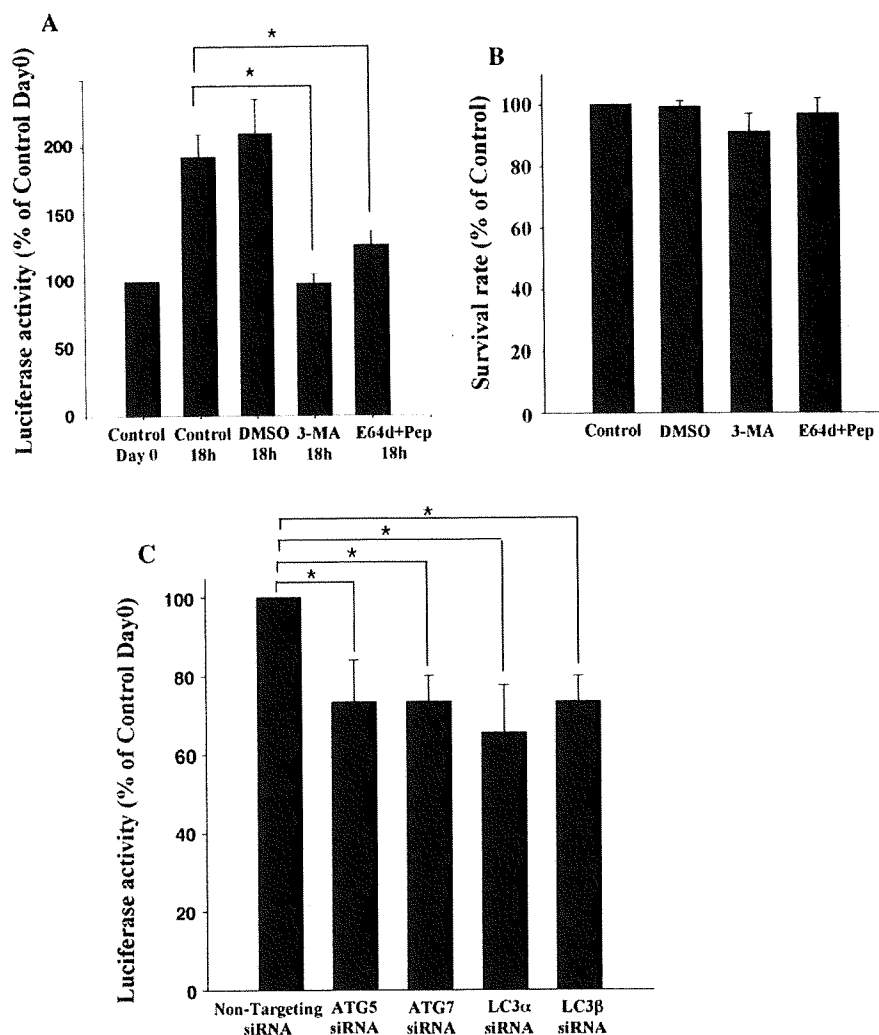


Fig. 1 Expression of autophagy is changed by presence or absence of HCV replicon. **a** Naïve Huh7 cells, Huh7/Rep-Feo cells, and Huh7/Rep-Feo treated with IFN α for 14 days were seeded on 30 mm dishes and incubated for 48 h. The cells were analyzed by a transmission electron microscope. Autophagosomes (arrow heads) were detected by transmission electron microscopy. **b** The number of autolysosomes in $100 \mu\text{m}^2$ of cytoplasm was counted by using transmission electron microscopy

Fig. 2 Inhibition of autophagy suppressed replication of HCV replicon. **a** Cells were treated with 3-methyladenine (3-MA) (10 mM) or a mixture of E64d (1 μ g/ml) and pepstatin A (Pep) (1 μ g/ml) for 18 h, the levels of replication of HCV replicon were assessed by luciferase assay. **b** Cells were treated with 3-methyladenine (10 mM), mixture of E64d (1 μ g/ml) and pepstatin A (1 μ g/ml) for 18 h. Cell proliferation reagent WST-1 was added to each well, and the cells were incubated for 1 more hour at 37°C. The absorbance was measured against a background control by microplates reader at 450 nm. The reference wavelength was 650 nm. **c** A combination of four chemically synthesized siRNA duplex molecules targeted to the human ATG5, 7, LC-3 α , LC-3 β mRNA sequence was transiently transfected into Huh7/Rep-Feo cells using a transfection reagent. siRNA targeted to enhanced green fluorescence protein was used as the control. Forty-eight hours after transfection, levels of HCV replication were analyzed by luciferase assay



Statistical analysis

Differences were compared using ANOVA. Basically *P* values less than 0.05 were considered as statistically significant.

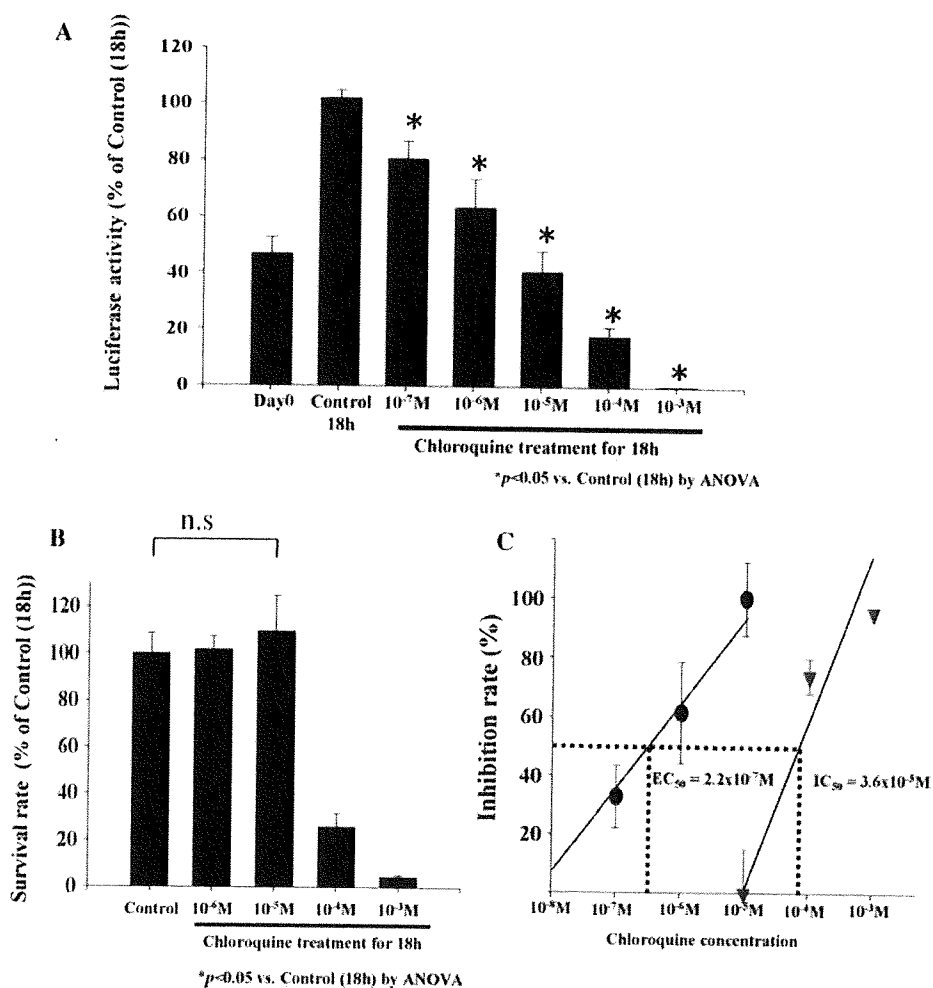
Results

The inhibition of autophagy suppressed replication of HCV replicon

We counted numbers of autophagosome and autolysosome in cells transduced with HCV replicon Rep-Feo by using electron microscopy. Double membrane vesicles with the morphology of autophagosomes were identified at 2.3 vacuoles/cells in naïve Huh-7 cells, while transfection of HCV replicon increased the number of vacuoles to about fourfold over untransfected Huh-7 cells (Fig. 1a, b).

Subsequent treatment of the cells with IFN α (100 U/ml) for 14 days to eliminate HCV replicon substantially decreased the autophagolysosome in cytoplasm of Huh7/Rep-Feo cells (Fig. 1a, b). These observations suggested that HCV replicon induces formation of autophagosomes. To clarify the role of autophagy on the replication of HCV, Huh7/Rep-Feo cells were treated with 3-methyladenine (10 mM) or a mixture of E64d (10 μ g/ml) and pepstatin A (10 μ g/ml) which inhibited autophagic protein degradation. Replication level of HCV replicon in cells was increased to about twofold after 18 h in control media, however incubation with 3-methyladenine completely blunted increases in replication of HCV replicon. Treatment with 3-methyladenine decreased the number of autophagosomes to about 19% of Huh7/Rep-Feo cells. Furthermore co-incubation with E64d and pepstatin A decreased replication of HCV replicon to about 66% of control (Fig. 2a). Next, WST-1 assay was performed to check the cytotoxicity of these drugs. Treatment with 3-methyladenine or a mixture of

Fig. 3 Effect of chloroquine on inhibition of HCV replication and cell viability. **a** Effect of chloroquine on replication of HCV replicon. Huh-7 Rep/Feo cells were seeded in 48-well plate and incubated with chloroquine (10^{-7} – 10^{-3} M) for 18 h. Replication levels of HCV replicon were determined by luciferase assay. Values are shown as percentages of the control cells. [$*P < 0.05$ vs. control (18 h) by ANOVA]. **b** Effect of chloroquine on proliferation of Huh-7 Rep/Feo cell lines in vitro. Cells seeded in 96-well plates were treated with 10^{-6} to 10^{-3} M of chloroquine. After 18 h, effects on cell proliferation were determined by WST-1 assay. [$*P < 0.05$ vs. control (18 h) by ANOVA]. **c** Calculation of EC_{50} and IC_{50} . Concentration of chloroquine inhibiting 50% of the replication of HCV replicon is shown as EC_{50} . IC_{50} is the concentration of chloroquine which inhibits 50% of the cell proliferation of Huh-7 Rep/Feo cells



E64d and pepstatin A did not affect cell viability (Fig. 2b). To clarify the role of autophagy induction in the replication of HCV, we suppressed the induction of autophagy by silencing autophagy-related genes (ATG5, ATG7, LC-3 α and LC-3 β) by siRNA transfection. Silencing of autophagy-related genes reduced the replication of HCV replicon to about 70% of control (Fig. 2c). Transfection with siRNA of autophagy related genes decreased the number of autophagosomes to about 30% of control. These results indicated that autophagy plays a pivotal role in replication of HCV.

Chloroquine inhibits the replication of HCV replicon

Next, we evaluated the anti-HCV effect of chloroquine, which is a lysosomotropic agent that raises intralysosomal pH and impairs autophagic protein degradation. To assess the effects of chloroquine on the intracellular replication of the HCV replicon, Huh7/Rep-Feo cells were cultured with various concentrations of chloroquine in the medium. The replication of the HCV replicon was

increased to about twofold within 18 h in the control media, however, which was suppressed by chloroquine in a dose-dependent manner (Fig. 3a). Next, cytotoxicity of chloroquine was analysed by WST-1 assays. Huh7/Rep-Feo cells treated with chloroquine showed no significant effect on cell viability in doses of lower than 10^{-5} M (Fig. 3b). However, incubation with 10^{-4} M of chloroquine reduced the cell viability to 25% of control. On the basis of the toxicity curve, the IC_{50} of the drug was calculated to be 3.6×10^{-5} M (Fig. 3c). The average EC_{50} of chloroquine was calculated as 2.2×10^{-7} M (Fig. 3c). The replication of HCV replicon was suppressed to nearly 40% of control at 10^{-5} M of chloroquine, which did not affect cell viability. These data indicated that chloroquine efficiently inhibited the replication of HCV replicon in the absence of toxic effect to cells at the concentration of 10^{-5} M. Accordingly, we used 10^{-5} M of chloroquine for the following study.

Next, we conducted the following assay to determine the synergistic inhibitory effect of chloroquine to IFN α on HCV replication. Treatment with chloroquine for 18 h

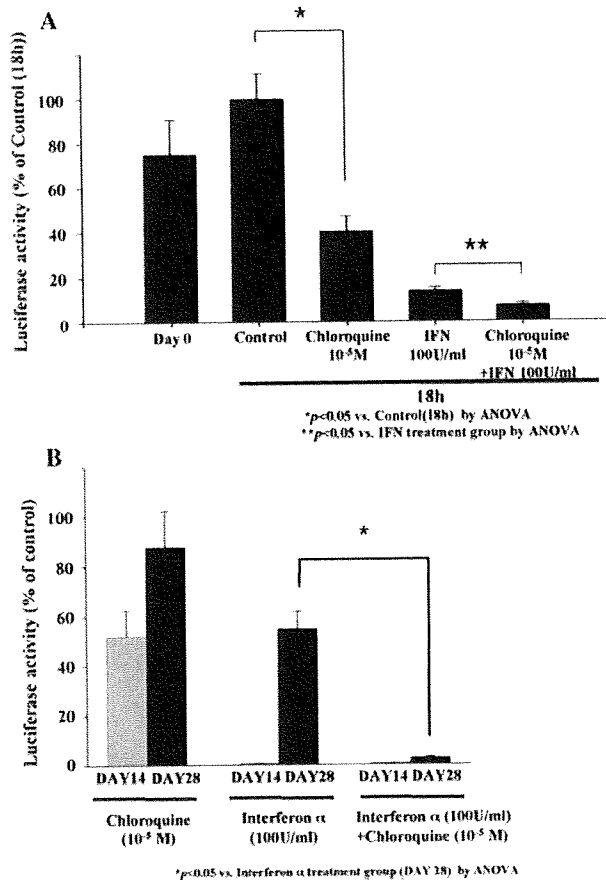


Fig. 4 Combination effect of chloroquine with IFN α on HCV replication. **a** Huh-7 Rep/Feo cells were treated with chloroquine (10⁻⁵ M) and/or IFN α (100 U/ml) for 18 h. Values are shown as percentages of the control cells [$*P < 0.05$ vs. control (18 h) by ANOVA, $**P < 0.05$ vs. IFN α treatment group by ANOVA]. **b** Assessment of re-propagation of HCV replicon after long term treatment of chloroquine and/or IFN α . Huh-7 Rep/Feo was incubated with chloroquine (10⁻⁵ M) and/or IFN α (100 U/ml) for 7 days, then drugs were removed from the medium and incubation continued for another 21 days. Luciferase assay was performed at the 7th and 21st days from cessation of drugs. Values are shown as percentages of the control cells [$*P < 0.05$ vs. IFN α treatment group (day 28) by ANOVA]

resulted in a significant decrease of HCV replicon to about 40% of control. On the other hand, incubation with IFN α for 18 h inhibited the replication of HCV replicon to the levels about 15% of controls as expected. However, co-incubation with 100U/ml of IFN α and 10⁻⁵ M of chloroquine further decreased HCV replication significantly (Fig. 4a).

To determine whether long-term chloroquine treatment inhibits post-treatment re-propagation of HCV replicon, we followed up luciferase activity of the cells at the 7th and 21st days after 7 days of treatment with chloroquine and/or IFN α (Fig. 4b). In HCV replicon cells treated by chloroquine, luciferase activities recovered to 53 and 88% on 7

and 21 days after cessation of treatment. In cells that were treated by IFN α , luciferase activity maintained background level for 7 days post-treatment. However, it reappeared in 21 days. In sharp contrast, co-incubation with IFN α and chloroquine for 7 days suppressed HCV replication for the extensive period up to 21 days, even in the absence of these drugs (Fig. 4b).

Anti-HCV effect of chloroquine independent of IFN signaling pathway

IFN-inducible double-stranded RNA-activated protein kinase R (PKR) plays a key antiviral role against hepatitis C virus [26, 27]. To elucidate the mechanisms of the inhibitory effect of chloroquine on HCV replication, phosphorylated PKR (P-PKR) was evaluated by western blotting analysis. P-PKR was detectable in cells treated with IFN α after 24 h; this increase in P-PKR expression peaked at 24 h after IFN α treatment and was reduced at 48 h (Fig. 5a). In contrast, P-PKR was not observed in cells treated with chloroquine at any time point.

Chloroquine blunts autophagic proteolysis in cells transfected with HCV replicon

It is reported that chloroquine disrupts lysosomal function, preventing effective autophagic protein degradation, leading to the accumulation of ineffective autophagosomes [28]. Therefore, we investigated if chloroquine led to the accumulation of autolysosomes as a result of suppression of proteolysis. We performed electron microscopic investigation to evaluate quantities of autophagosomes and autolysosomes. Ultrastructural analysis identified 0.94 ± 0.1 vacuoles/100 μm^2 of autolysosomes in control cells; however, treatment with chloroquine increased the number of autolysosomes dramatically to about 13-fold over control (Fig. 5b). Furthermore, the molecular form of LC3 protein of the cells, which is a component of autophagosomes, was examined by western blot analysis to ensure that chloroquine treatment leads to the accumulation of autophagosomes and autolysosomes. As shown in Fig. 5c, immunopositive protein bands for LC3-I and LC3-II forms were clearly evident in control cells. After chloroquine treatment, LC3-II expression increased at 4 h (Fig. 5c) to about threefold over control without enhancing LC3-I expression, and at 8 h (Fig. 5c) LC3-II expression was further enhanced. Finally, we evaluated turnover of the long-lived protein leucine, which was mainly degraded by autophagy. Huh7/Rep-Feo cells were labeled with [¹⁴C]leucine for 24 h, and degradation of [¹⁴C]leucine in cells treated with or without chloroquine was measured. Chloroquine treatment decreased degradation of leucine to 76% of control, indicating that chloroquine blunts degradation of proteins via an autophagic